

AD-A104 582

SRI INTERNATIONAL MENLO PARK CA  
THE CHEMICAL VAPOR DEPOSITION OF IRIDIUM, (U)

JUL 81 J B MOONEY, R T REWICK, D L HAYNES

F/G 9/1

N00014-79-C-0880

NL

UNCLASSIFIED

for I  
AD-A  
0 5-82

END  
DATE  
10-81  
DTIC

**DMC FILE COPY**

**AD A104582**

**LEVEL**



## **THE CHEMICAL VAPOR DEPOSITION OF IRIDIUM.**

*(Signature)*  
**Final Report**

*(Signature)*  
**June 1981**



*(Signature)*  
**By: John B. Mooney, Senior Research Chemist  
Engineering Sciences Laboratory**

**Robert T. Rewick, Physical-Inorganic Chemist  
Daniel L. Haynes, Chemist  
Thomas E. Gray, Chemist  
David M. Vandenberg, Chemist  
Physical Chemistry Department**

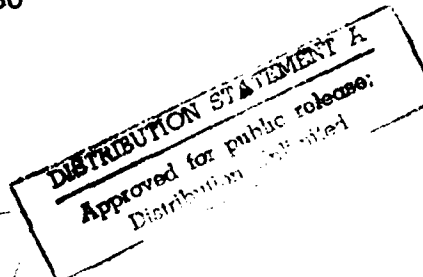
**Prepared for:**

**Scientific Officer, NRL Code 5220  
Naval Research Laboratories  
4555 Overlook Avenue  
Washington, D.C. 20375**

**Attn: Mr. Howard Lessoff**

*15-*  
**Contract/N00014-79-C-0880**

**SRI Project 1013**



**SRI International  
333 Ravenswood Avenue  
Menlo Park, California 94025  
(415) 326-6200  
Cable: SRI INTL MPK  
TWX: 910-373-1246**



**81 7 31 068**

## UNCLASSIFIED

SECURITY CLASSIFICATION OF THIS PAGE (When Data Entered)

REPORT DOCUMENTATION PAGE		READ INSTRUCTIONS BEFORE COMPLETING FORM
1. REPORT NUMBER	2. GOVT ACCESSION NO.	3. RECIPIENT'S CATALOG NUMBER
	AD-A104	582
4. TITLE (and Subtitle)	5. TYPE OF REPORT & PERIOD COVERED	
THE CHEMICAL VAPOR DEPOSITION OF IRIDIUM	Final Report	
7. AUTHOR(s)	6. PERFORMING ORG. REPORT NUMBER	
J.B. Mooney, R.T. Rewick, D.L. Haynes, T.E. Gray, D.M. Vandenberg	SRI Project 1013	
9. PERFORMING ORGANIZATION NAME AND ADDRESS	8. CONTRACT OR GRANT NUMBER(s)	
SRI International 333 Ravenswood Avenue Menlo Park, California 94025	Contract N00014-79-C-0880	
11. CONTROLLING OFFICE NAME AND ADDRESS	10. PROGRAM ELEMENT, PROJECT, TASK AREA & WORK UNIT NUMBERS	
Naval Research Laboratories 4555 Overlook Avenue Washington, D.C. 20375	12. REPORT DATE	
14. MONITORING AGENCY NAME & ADDRESS (if diff. from Controlling Office)	13. NO. OF PAGES	
	July 1981	28
16. DISTRIBUTION STATEMENT (of this report)	15. SECURITY CLASS. (of this report)	
	Approved for public release; Distribution Unlimited	
17. DISTRIBUTION STATEMENT (of the abstract entered in Block 20, if different from report)	15a. DECLASSIFICATION/DOWNGRADING SCHEDULE	
18. SUPPLEMENTARY NOTES	S DTIC ELECTED SEP 25 1986 H	
19. KEY WORDS (Continue on reverse side if necessary and identify by block number)		
20. ABSTRACT (Continue on reverse side if necessary and identify by block number)		
The preparation of iridium films for thermionic cathodes by chemical vapor deposition was studied. The deposition from IrCl <sub>3</sub> /H <sub>2</sub> /CO atmospheres was very inefficient; however, iridium was deposited from IrF <sub>3</sub> /H <sub>2</sub> /CO at 465°C & 25°C with reasonable efficiency.		
The majority of the deposits were porous or loose powders. An attempt to deposit iridium on a substrate designed to produce a microporous film was unsuccessful because of the poor throwing-power of the process.		

## ABSTRACT

The preparation of iridium films for thermionic cathodes by chemical vapor deposition was studied. The deposition from  $\text{IrCl}_3/\text{H}_2/\text{CO}$  atmospheres was very inefficient; however, iridium was deposited from  $\text{IrF}_6/\text{H}_2/\text{CO}$  at  $465^\circ\text{C} \pm 25^\circ\text{C}$  with reasonable efficiency.

The majority of the deposits were porous or loose powders. An attempt to deposit iridium on a substrate designed to produce a micro-porous film was unsuccessful because of the poor throwing-power of the process.

Accession For	<input checked="" type="checkbox"/>
NTIS GRA&I	<input type="checkbox"/>
DTIC TAB	<input type="checkbox"/>
Unannounced	<input type="checkbox"/>
Justification	<i>Per FL</i>
By	<i>surface</i>
Distribution/	
Availability Codes	
Anti-Spy	
Dist	Special
A	

## CONTENTS

ABSTRACT.....	ii
LIST OF ILLUSTRATIONS.....	iv
LIST OF TABLES.....	v
I    INTRODUCTION.....	1
II   EXPERIMENTAL DETAILS.....	3
A.    Apparatus.....	3
B.    Materials.....	7
III  RESULTS.....	9
A.    Deposition from IrCl <sub>3</sub> .....	9
B.    Deposition from IrF <sub>6</sub> .....	9
C.    Effect of Temperature.....	11
D.    Substrate Type.....	15
E.    IrF <sub>6</sub> Exposure.....	16
F.    Effect of Carrier Gas Composition and Flow Rate.....	17
G.    Effect of Low Pressure.....	18
H.    Nature of the Deposit.....	18
I.    Elemental Analysis.....	22
J.    Deposition on Silicon Microstructures.....	22
IV   DISCUSSION.....	24
A.    Iridium Deposition from IrCl <sub>3</sub> .....	24
B.    Iridium Deposition from IrF <sub>6</sub> .....	24
REFERENCES.....	26

## ILLUSTRATIONS

1	Schematic Diagram of Iridium Chemical Vapor Deposition Apparatus.....	4
2	Chemical Vapor Deposition Apparatus.....	5
3	Assembled Apparatus with Vaporizer in Place.....	6
4	Sticking Efficiency for Iridium Deposition on Copper from IrF <sub>6</sub> as a Function of Temperature.....	15
5	Dendrite Iridium Deposit (Run 33 in Table 4).....	20
6	5000X SEM Photograph of Iridium Deposit on Copper Substrate (Run 16 in Table 3).....	20
7	5000X SEM Photograph of Iridium Deposit on Copper Substrate (Run 5 in Table 3) Before Removal.....	21
8	2000X SEM Photograph of Iridium Deposit (Back Side, Run 5 in Table 3) After Removal from Copper Substrate.....	21
9	Deposition on Silicon Microstructure.....	23

TABLES

1 Preparation of IrF <sub>6</sub> .....	8
2 Summary of Iridium Deposition Results Using IrCl <sub>3</sub> .....	10
3 Initial Iridium Deposition Results from IrF <sub>6</sub> .....	12
4 Iridium Deposition Results from IrF <sub>6</sub> .....	13

## I INTRODUCTION

This report summarizes the results of an investigation of a method for the production of thin films of iridium by chemical vapor deposition (CVD) with the objective of controlling crystallographic orientation.

The need for ultra-long-life ( $> 10^6$  hour) traveling wave tubes for satellite communications has stimulated a resurgence of interest in dispenser cathodes (Schroff, 1978; Longo, 1978; Smith, 1978). The conventionally accepted types are made of porous tungsten impregnated with barium calcium aluminates (Levi, 1955; Brodie and Jenkins, 1956). The emission capability of the dispenser cathode gradually decreases during its lifetime at a rate strongly dependent upon the cathode's operating temperature (Longo, 1978). Related experiments have shown that this decay is associated with a decline in the rate at which barium is supplied to the surface (Brodie and Jenkins, 1957a; Rittner et al., 1957) and with changes in the physical-chemical structure of the cathode surface. Scanning electron micrographs have shown that not only does the chemical composition of the pore ends and the bulk material undergo alteration, but the crystal structure of the tungsten (Maloney, 1978; Sickafus, 1978) is also affected. Emission micrographs of the cathode surface show a marked patchiness (Brodie and Jenkins, 1957b; Tuck, 1978), with the more intense emission originating at the pore endings--at least at the beginning of life.

Recently, there have been studies of iridium as a base metal for dispenser cathodes, at the Naval Research Laboratory (NRL) (Thomas et al., in press) and at Varian (Falce, 1978). The various properties of iridium that can influence cathode operation were discussed by Thomas et al. They found that, as with other materials (Weissman and Kinter, 1963), crystallographic orientation influences the thermionic work function, and, in randomly oriented, large-grained films, is responsible for

"patchy" emission. Oriented polycrystalline films can be produced by vapor deposition (Thomas et al., in press; Bauer, 1962; Powell et al., 1966; Yang and Hudson, 1967; McMurray et al., 1965).

Our investigation revealed that the deposition of iridium using  $\text{IrCl}_3$  as a source was very inefficient even in the presence of  $\text{H}_2/\text{CO}$ .  $\text{IrF}_6$  was a more efficient source, and we could deposit iridium layers over a substrate temperature range of  $400^\circ\text{C}$  to  $500^\circ\text{C}$ , with a sharp peak in the deposition efficiency at  $465^\circ \pm 25^\circ\text{C}$ .

Depositions up to  $50-\mu\text{m}$  thick were obtained. The depositions were porous and often nonadherent powders. No evidence of preferred orientation was found.

## II EXPERIMENTAL DETAILS

### A. Apparatus

A schematic view of the stainless-steel-and-glass iridium chemical-vapor-deposition apparatus is shown in Figure 1. The volatile iridium source could be supplied from either the  $\text{IrCl}_3$  or  $\text{IrF}_6$  vaporizer as shown. The carrier gas, consisting of either argon (Ar), hydrogen ( $\text{H}_2$ ), or carbon monoxide (CO), or mixture, was metered through the appropriate vaporizer from calibrated flowmeters. Deposition experiments were usually conducted at atmospheric pressure, but a Cartesian diver pressure regulator was sometimes used to investigate subambient conditions. The substrate, consisting of a freshly etched or cleaned metallic specimen, was placed on a graphite susceptor containing a thermocouple well and centered in position between radio frequency (RF) induction coils (Lepel Model 1-2.5). The flow stream containing volatilized iridium struck the heated surface of the specimen through a cone-shaped glass impinger located about 1.5-mm above the specimen surface. The wall temperature of the reactor was maintained by a hot-air gun for  $\text{IrCl}_3$  experiments and by cold water for  $\text{IrF}_6$  experiments. A photograph of the assembled apparatus with the  $\text{IrF}_6$  vaporizer in place is shown in Figures 2 and 3. Volatile iridium species were generated from  $\text{IrCl}_3$  by flowing the carrier gas (mixtures of argon, carbon monoxide, and hydrogen) through a heated sample of the powder in the vaporizer shown in Figure 1. The exact nature of the volatile iridium species was unknown, but a iridium carbonyl chloride such as  $\text{IrCOCl}_2$  was a likely candidate. To avoid deposition of iridium on cold wall surfaces, the lines following the  $\text{IrCl}_3$  vaporizer were heated.

The vaporizer containing  $\text{IrF}_6$  was transferred to the vapor phase by passing the carrier gas (usually a mixture of argon and carbon monoxide) through the U-tube maintained at low temperature. The mass flow rate of

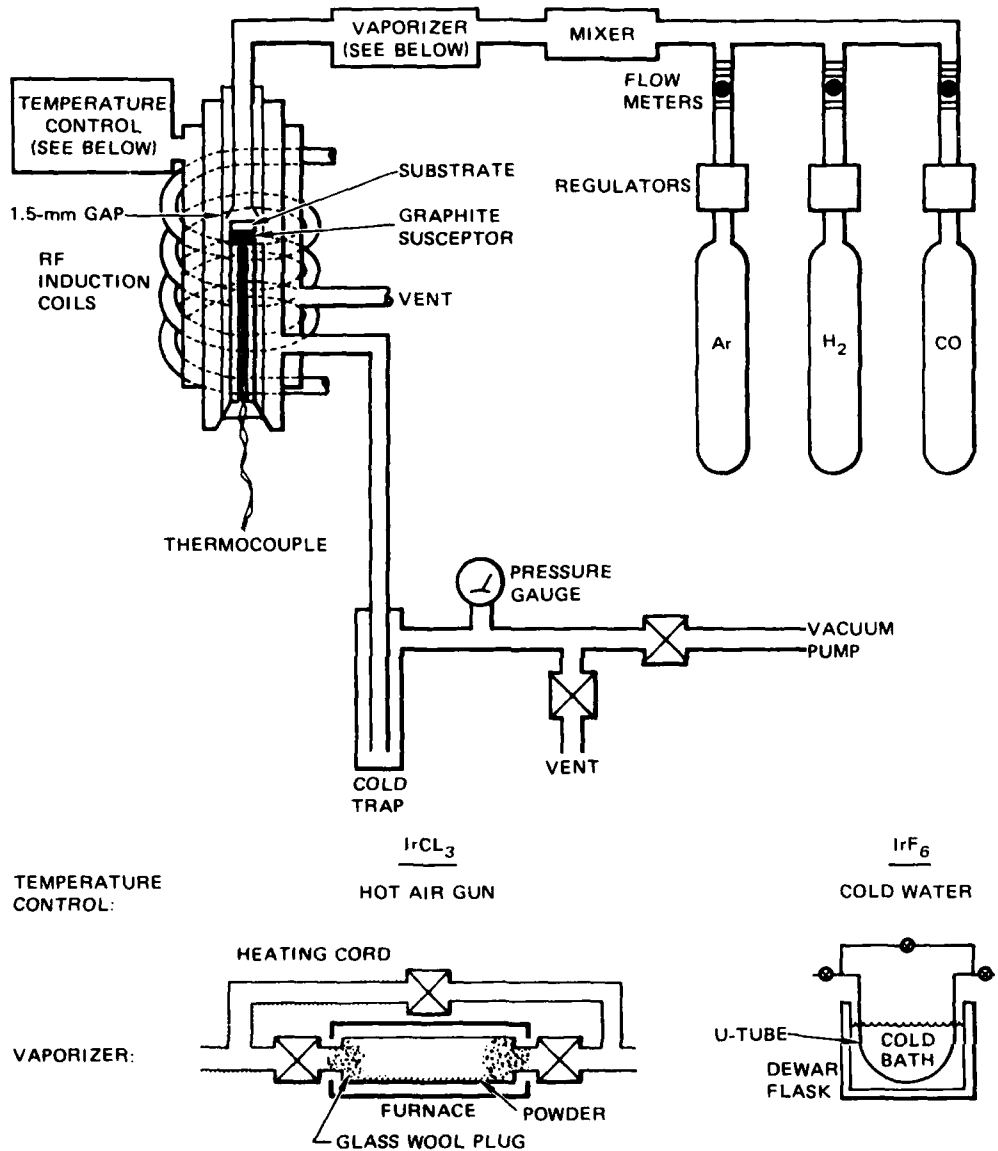


FIGURE 1 SCHEMATIC DIAGRAM OF IRIDIUM CHEMICAL VAPOR DEPOSITION APPARATUS

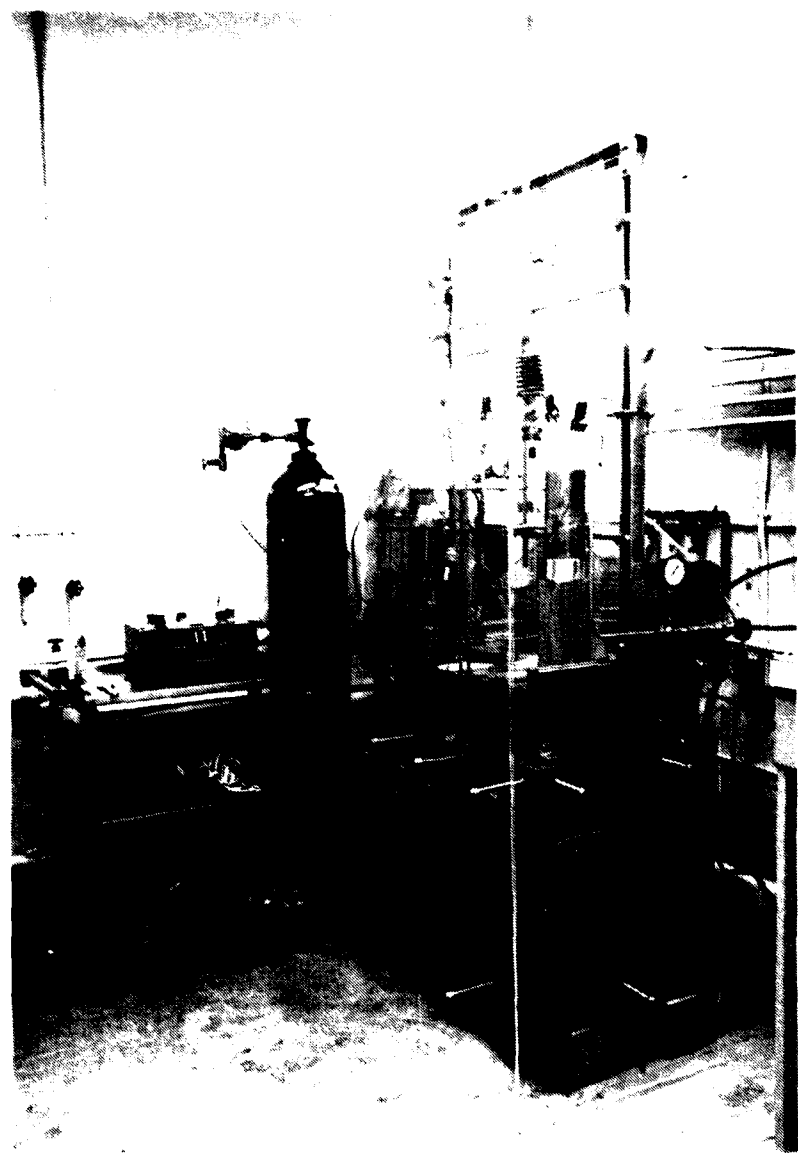


FIGURE 2 - CHEMICAL VAPOR DEPOSITION APPARATUS

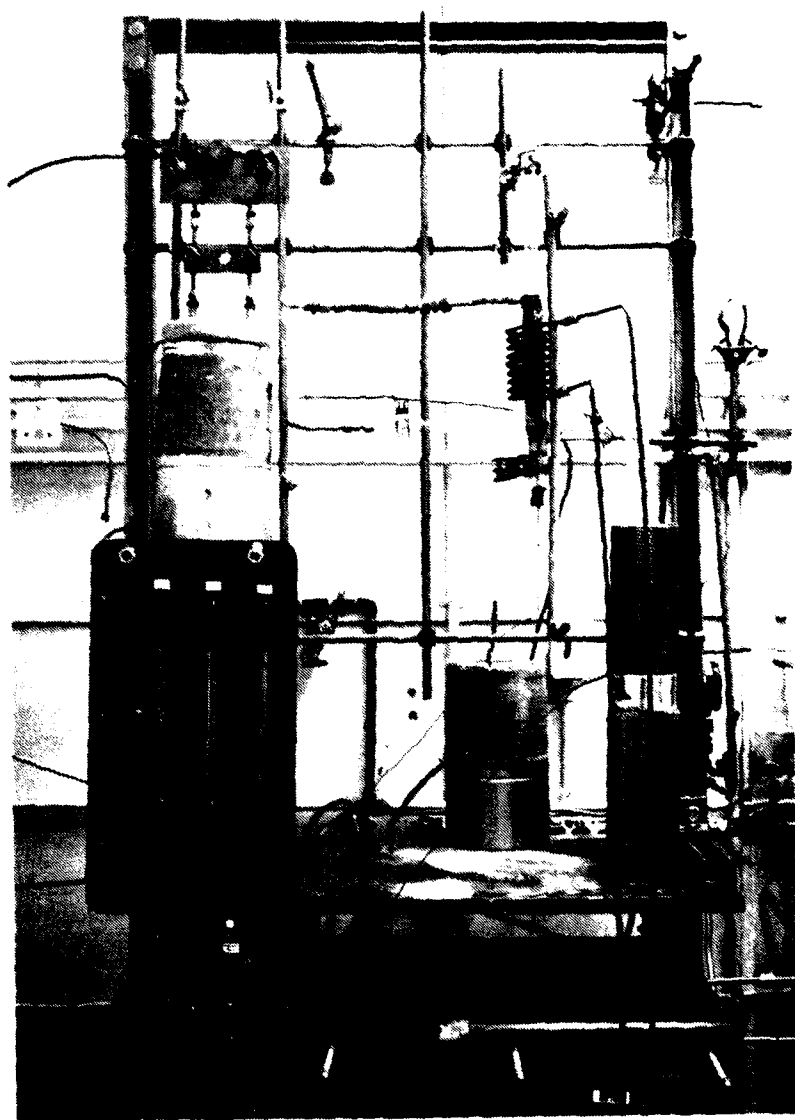


FIGURE 3 ASSEMBLED APPARATUS WITH VAPORIZER IN PLACE

$\text{IrF}_6$  can be estimated from the volumetric flow rate of the carrier gas and the known vapor pressure/temperature relationship for  $\text{IrF}_6$ . Since vapor saturation was not achieved under our flow conditions, we calculated the actual  $\text{IrF}_6$  mass flow rate by weighing the U-tube before and after the deposition experiment. To avoid losses of  $\text{IrF}_6$  to hot wall surfaces, the reactor walls were cooled with cold water.

#### B. Materials

Amorphous  $\text{IrCl}_3$  was obtained from Alpha Products in sealed glass ampules. All transfers of the powder were conducted in the inert atmosphere ( $\text{N}_2$ ) of a dry box. To prepare  $\text{IrF}_6$ , a section of 0.030-inch (0.75 mm) diameter iridium wire (99.5 percent purity from Englehard Industries) was burned in elemental fluorine (280 torr) in a Monel® vessel maintained at  $-196^\circ\text{C}$ . Under these conditions, combustion of iridium proceeds to  $\text{IrF}_6$  in greater than 90 percent conversion (Table 1). The volatile product was then distilled into the tared U-tube and stored at  $-78.5^\circ\text{C}$ . During a deposition experiment, the U-tube was attached to the CVD apparatus and maintained at the desired temperature with a slush bath, usually  $\text{LN}_2$ /acetonitrile ( $-46.5^\circ\text{C}$ ).

The suitability of a variety of metallic substrates for the deposition of iridium was investigated during the course of this study. The materials included molybdenum, copper, iridium-coated copper, silicon,  $\text{SiO}_2$ -coated silicon, and copper-coated silicon. In general, the specimens were 0.625-inch (1.5625 cm) diameter disks, about 0.005 to 0.010-inch (0.125 to 0.25 mm) thick, and cleaned by standard acid etching or polishing techniques. Each sample was weighed to  $\pm 0.2$  mg before and after the experiment to determine the weight of iridium deposited. The nature of the deposit on selected specimens was characterized by scanning electron microscopy (SEM), X-ray fluorescence (XRF), and X-ray diffraction (XRD) analysis.

Table 1

PREPARATION OF  $\text{IrF}_6$   
 $(\text{Ir} + 3\text{F}_2 \rightarrow \text{IrF}_6)$

Run	Reactants			Product	
	Fluorine (mole)	Iridium * (mole)	Iridium Consumed * (wt%)	$\text{IrF}_6$ (mole)	Conversion † (wt%)
1	0.0510	0.0161	88.8	0.0130	91.2
2	0.0597	0.0162	92.6	0.0126	84.5
3	0.0594	0.165	93.6	0.0117	76.0
4	0.0616	0.0166	93.5	0.0146	94.2
5	0.0598	0.0165	93.2	0.0142	92.4
6	0.0595	0.0167	(51.2)‡	0.0060	(69.5)‡
7	0.0599	0.0165	93.1	0.0143	93.0
8	0.0608	0.0163	93.1	0.0167	110.3
9	0.0603	0.0165	93.7	0.0137	88.7
10	0.0600	0.0164	93.5	0.0140	91.4
11	0.0603	0.0164	93.2	0.0144	94.2
12	0.0436	0.0123	91.0	0.0105	93.4
Average			92.7		91.8

\* 0.030-inch diameter wire (99.5 percent purity).

† Based on weight of iridium consumed.

‡ Wire broke (not included in average).

### III RESULTS

#### A. Deposition from IrCl<sub>3</sub>

The important parameters concerning the efficient deposition of iridium from IrCl<sub>3</sub> included vaporizer and substrate temperatures and carrier-gas composition and flowrate. The results from these studies, summarized in Table 2, demonstrate that no more than about 2.5 mg of iridium can be deposited on a molybdenum or copper substrate in the form of isolated iridium patches as detected by SEM/XRF surface analysis. Specifically, we observed that conditions that fostered the generation of a volatile iridium species (150°C to 200°C in the presence of H<sub>2</sub>/CO) also fostered the reduction of IrCl<sub>3</sub> to the metal. In nearly all attempts to volatilize iridium from IrCl<sub>3</sub> in the presence of H<sub>2</sub>/CO, but especially with hydrogen, theoretical conversion of the chloride to finely divided pyrophoric iridium metal was observed. The small fraction of volatile iridium species generated during reduction to the metal, responsible for the iridium deposits observed on the molybdenum and copper substrates, appeared to decompose on wall and substrate surfaces heated above 300°C.

#### B. Deposition from IrF<sub>6</sub>

Our experimental approach to optimizing conditions for the deposition of iridium from IrF<sub>6</sub> has entailed a detailed evaluation of these parameters: substrate type, temperature, pressure, IrF<sub>6</sub> concentration, flow rate, and presence of hydrogen and CO in the carrier stream. Results from these studies are described below.

Table 2  
SUMMARY OF IRIDIUM DEPOSITION RESULTS USING  $\text{IrCl}_3$

Run Number	Sample*	Carrier Gas		Temperature Conditions ( $^{\circ}\text{C}$ )			Run Time (h)	Sample Weight Change (mg)	Parameter Studied	Notes
		Gas Composition (volume percent)	Flow Rate ( $\text{cm}^3/\text{min}$ )	$\text{IrCl}_3$ Lines	Transfer Wall	Reactor Wall				
1	Mo	30 CO/70 Ar	200	150 <sup>†</sup>	175	175	880	5.0	-0.8	Impinger
2	Mo	30 CO/70 Ar	200	249	175	175	895	5.1	+1.3	$\text{IrCl}_3$ Temp.
3	Mo	60 CO/40 Ar	200	250	175	175	830	5.0	-0.7	Co Conc.
4	Mo	33 CO/67 H <sub>2</sub>	200	175	175	180	885	5.0	+0.6	
5	Cu	33 CO/67 H <sub>2</sub>	200	173	175	185	880	5.0	+0.1	Cu Sample
6	Cu	30 CO/70 Ar	200	242 <sup>†</sup>	175	180	885	5.0	-0.4	Repeat No. 2
7	Cu	30 CO/70 Ar	200	247	175	170	530	5.0	-0.8	Sample Temp.
8	Cu	30 CO/70 Ar	200	250	175	150	337	5.0	0	Sample Temp.
9	Cu	30 CO/70 Ar	500	242 <sup>†</sup>	175	170	350	5.0	-0.6	Flow Rate
10	Cu	30 CO/70 Ar	200	245 <sup>†</sup>	175	175	346	5.1	+0.2	Repeat No. 8
11	Cu	28 CO/69 Ar/3 H <sub>2</sub> O	200	250 <sup>†</sup>	175	175	345	5.3	+2.4	Effect of H <sub>2</sub> O
12	Cu	28 CO/69 Ar/3 H <sub>2</sub> O	200	145	150	165	302	5.0	+1.1	Sample Temp.
13	Cu	28 Cu/69 Ar/3 H <sub>2</sub> O	200	152 <sup>†</sup>	163	163	296	5.2	-0.1	Repeat No. 12
									3,6	

\* Metal disk 0.625-inch (15.9 mm) diameter  $\times$  0.005-inch (0.127 mm) thick.  
† Fresh  $\text{IrCl}_3$  sample.

NOTES:

1. SEM/XRF Analysis isolated particles of iridium.
2.  $\text{IrCl}_3$  reduced to iridium metal.
3. Silver-colored coating on sample.
4. SEM/XRF Analysis isolated particles of iridium; high nickel, iron.
5. SEM/XRF Analysis higher concentration of iridium particles; high chlorine.
6. SEM/XRF Analysis nearly uniform iridium film; some particles.

### C. Effect of Temperature

Initial screening experiments to optimize deposition temperature were conducted in the range 308°C - 915°C on a copper substrate. Above 700°C, the amount of iridium deposited (above 30 mg) was essentially independent of temperature, flow rate, or IrF<sub>6</sub> concentration. Below 700°C, temperature played a dramatic role on the amount of adherent iridium deposited. The relationship between temperature and iridium deposition is best compared to the deposition efficiency of IrF<sub>6</sub>, which is defined as substrate weight gain/total IrF<sub>6</sub> exposure. As shown in Table 3, initial IrF<sub>6</sub> exposures were not constant and varied over a large range; this deficiency was corrected in later experiments. Initial results suggested that maximum iridium deposition efficiency occurred over a narrow temperature range; at ~489°C, nearly 20 percent of the exposed IrF<sub>6</sub> was deposited as iridium on the copper substrate. A ± 10°C variation from this temperature reduced the deposition efficiency to less than 5 percent. In these early experiments, the reported temperatures are that of the graphite susceptor. More accurate temperature measurements of the substrate surfaces were achieved by positioning the thermocouple to contact the sample. Temperature measurements at this position (Table 4) were about 20°C to 40°C cooler than those given in Table 3.

As shown in Table 4, we focus on temperature conditions near 450°C to optimize iridium deposition efficiency from IrF<sub>6</sub>. The results, plotted in Figure 4, demonstrate a narrow range temperature dependence for maximum efficiency, which peaks at about 465°C.

Because of the high radiant output from the heated graphite susceptor, reactor wall temperatures were difficult to control by air cooling, and varied between about 40°C to 190°C. Because the hot walls provided another sink for IrF<sub>6</sub> decomposition, more efficient cooling was provided by flowing tap water through the cooling jacket, which maintained the wall surface at about 18°C.

Table 3  
INITIAL IRIDIUM DEPOSITION RESULTS FROM IrF<sub>6</sub>

Run Number	Substrate	Carrier Gas	Gas Composition (vol %)	IrF <sub>6</sub>			Temperature (°C)	Substrate Weight Gain (mg)	Sticking Efficiency (%)	Nature of Deposit (see notes)	
				Flow Rate (cm <sup>3</sup> /min)	Total Exposure (sec)	Mass Flow Rate (mg/h)				Visual	XRD
1	Ir/Cu	82 Ar/18 CO	73	-78.5	1266	60	474	40	32.6	2.6	Black
2	Ir/Cu	82 Ar/18 CO	73	-78.5	135	8	308	18	2.0	1.5	Spotty black
3	Ir/Cu	82 Ar/18 CO	73	-78.5	21	1	504	18	0.9	4.3	No visible deposit
4	Ir/Cu	82 Ar/18 CO	73	-46.5	317	79	470	18	4.3	1.4	Fairly uniform grey with some black patches
5	Cu	82 Ar/18 CO	73	-46.5	501	123	493	18	84.1	16.8	Adherent, grey
6	Cu	82 Ar/18 CO	73	-46.5	380	91	308	18	5.0	1.3	Grey/black, hygroscopic
7	Cu	82 Ar/18 CO	73	-46.5	122	31	415	18	2.1	1.7	Adherent, light grey
8	Cu	82 Ar/18 CO	73	-46.5	---	---	577	23	0.3	---	Adherent, silver
9	Cu	82 Ar/18 CO	73	-46.5	1559	390	613	18	6.6	0.4	Loose, dark grey
10	Cu	82 Ar/18 CO	73	-46.5	1938	473	443	18	12.5	0.6	Loose, dark grey
11	Cu	82 Ar/18 CO	73	-46.5	183	46	732	18	10.9	6.0	Light coating, lumps
12	Cu	73 Ar/27 CO	73	-46.5	916	250	488	18	71.5	7.8	Loose, silver/black
13	Cu	100 Ar	50	-46.5	113	28	499	18	2.9	2.6	Loose, grey/black
14	Cu	82 Ar/18 CO	73	-78.5	-13	-0.8	512	18	0.1	---	No visible deposit
15	Cu	82 Ar/18 CO	73	-78.5	3019	163	553	18	86.5	2.9	Loose, grey/black
16	Cu	82 Ar/18 CO	73	-46.5	1128	282	489	18	224.4	19.9	Adherent, grey/black
17	Cu	82 Ar/18 CO	73	-46.5	227	56	580	18	6.1	2.7	Loose, grey/silver
18	Cu	82 Ar/18 CO	73	-46.5	125	31	486	18	7.6	6.1	Adherent, grey/black
											11

\* Adherent deposit.

<sup>a</sup> Weight gain/Total IrF<sub>6</sub> exposure.

NOTES:

1. Clusters and needles of iridium.
2. Mostly 1-mm particles with some 7.5-mm lumps.
3. Mostly 2.5-mm particles with some 10-mm clusters.
4. Broad-peaked iridium pattern (small particle size); unknown impurity.
5. Very thin coating, perhaps film.
6. Coating too thin to measure iridium pattern.
7. Thin film with cracks.
8. Thick film with cracks.
9. Strong iridium with sharp peaks; no evidence for preferred orientation.
10. Nonhomogeneous film surface with some larger clusters.
11. Hostile 4-mm particles with some larger clusters.

Table 4  
IRIDIUM DEPOSITION RESULTS FROM IrF<sub>6</sub>

Run Number	Substrate	Carrier Gas		IrF <sub>6</sub>			Sample Weight Gain (mg)	Substrate Weight Gain (mg)	Sticking Efficiency (%)	Nature of Deposit (see notes)	
		Gas Composition (vol. %)	Flow Rate (cm <sup>3</sup> /min)	Temp. (°C)	Total Exposure (mg)	Mass Flow Rate (mg/h)				Visual	SEM
17	Cu	60 Ar/40 CO	100	-46.5	520	130	490	18	47.1	9.1	Coherent grey/black film, some fell off when removing disk from apparatus.
20	Cu/Si	60 Ar/40 CO	100	-46.5	412	103	484	18	34.6	16.6	Silver/grey spotty deposit plus powder. Sample does not cover entire disk.
21	Cu	60 Ar/40 CO	100	-46.5	415	204	435	18	46.2	11.1	Nonuniform silver/grey deposit plus loose powder.
22	Cu	60 Ar/40 CO	100	-46.5	388	97	413	18	1.9	0.5	Light covering silver/black adherent plus fine powder.
23	Cu	60 Ar/40 CO	100	-46.5	285	70	474	18	2.7	0.9	Silver/black adherent + loose powder.
24	Cu	60 Ar/40 CO	100	-46.5	194	48	533	18	0	0	Thin silver/black adherent plus loose powder.
25	Cu	60 Ar/40 CO	100	-46.5	155	39	330	18	3.8	2.5	Thin metallic silver deposit; no loose powder.
26	Cu	82 Ar/18 CO	73	-46.5	166	42	437	18	0	0	No change of color of Cu disk, so little if any deposited.
27	Cu	82 Ar/18 CO	73	-46.5	315	74	436	15	35.6	11.3	Dark to light grey, mostly adherent, small amount of loose particulate.
28	Cu	82 Ar/18 CO	73	-46.5	315	79	469	15	-1.5	--	Center of disk dark blue/purple small amount loose particles.
29	Cu	82 Ar/18 CO	73	-46.5	398	96	402	15	1.4	0.4	Very thin dark purple film, adherent.
30	Cu	82 Ar/18 CO	73	-46.5	358	95	419	15	45.8	12.8	Light to dark grey adherent film.
31	Cu	82 Ar/18 CO	73	-46.5	295	74	370	15	8.3	2.8	Medium grey to metallic silver; adherent. Some loose particulate.
32	Cu	82 Ar/18 CO	73	-46.5	217	54	402	15	11.2	5.2	Light to medium grey adherent.
33	Cu	82 Ar/18 CO	73	-46.5	230	53	450	16	33.6	14.6	Medium grey, uniform and mostly adherent, small amount of loose particles.
34	Cu	82 Ar/18 CO	73	-46.5	129	29	478	16	26.2	20.3	Dark grey, uniform and mostly adherent. Moderate amount of loose particles.
35	Cu	82 Ar/18 CO	73	-46.5	214	54	506	15	11.1	5.2	Patchy dark grey, adherent.
36	Cu	82 Ar/18 CO	73	-46.5	194	48	485	15	13.3	6.9	Dark grey, adherent.
37	Cu	88 Ar/12 CO	75	-46.5	188	47	478	16	2.2	1.2	Medium to dark grey adherent with no loose particulate.
38	Cu	82 Ar/18 CO	73	-23	831	208	470	19	46.2	5.6	Mostly uniform dark grey adherent with large amount of loose particulate.
39	Cu	82 Ar/18 CO	73	-78.5	0	0	464	15	0	0	Uniform shiny silver, adherent--very thin.

Table 4 (concluded)

Run Number	Substrate	Carrier Gas (vol %)	Flow Rate (cm <sup>3</sup> /min)	IrF <sub>6</sub>			Sample (At Surface) Weight (mg)	Substrate Weight Gain (mg)	Sticking Efficiency <sup>a</sup> (%)	Nature of Deposit (see notes)		
				Gas Composition (vol %)	Temp. (°C)	Total Exposure (mg)				Visual	SEM	XRD
40	Cu	82 Ar/18 CO (0.30 atm)	?	-46.5	1278	399	485	14	24.5	1.9	Medium to light grey adherent, heavier on one side of disk, small amount of loose particulate.	
41	Cu	82 Ar/18 CO (0.096 atm)	?	-78.5	-56?	0	472	14	0	0	Cu discolored yellow and grayish with rough texture.	
42	Cu	82 Ar/18 CO	?	-78.5	20	5	468	14	0.4	2.0	Cu discolored with thin medium grey adherent. Darker spot in middle. Very small amount loose particulate.	
43	Cu	82 Ar/18 CO	?	-64	107	27	466	14	0	0	Very uniform light to medium grey adherent. Very small amount of loose particulate. Very thin deposit.	
44	Cu	82 Ar/18 CO (0.30 atm)	?	-63.5	20	5	467	14	0.1	0.5	Cu discolored mottled. Very small amount loose particulate.	
45	Cu	82 Ar/18 CO	73	-78.5	10	0.67	480	14	0	0	No deposit. No particulate.	
46	Cu	82 Ar/18 CO	73	-46.5	595	50	472	13	33.4	5.6	Dark grey adherent. Small amount loose particulate and a few lumps.	
47	Cu	82 Ar/18 CO	73	-46.5	441	37	486	13	56.7	12.9	Dark grey in middle surrounded by light grey. Lumpy with moderate amount of loose particulate.	
48	Cu	82 Ar/18 CO	73	-46.5	457	38	465	13	69.8	15.3	Dark grey, lumpy adherent with light grey spots in middle. Large amount loose particulate.	
49	Cu	82 Ar/18 Hz	73	-46.5	138	34.5	449	13	0	0	No adherent. Large amount loose flakes.	
50	Cu	82 Ar/18 CO	220	-46.5	811	162	471	13	32.1	4.0	Dark grey adherent. Smooth on out- side, rough in middle. Moderate amount loose particulate.	
51	Cu coated contoured silicon	82 Ar/18 CO	73	-46.5	820	68	465	13	10.5	1.3	Splotchy light and dark grey adherent. Large amount loose particulate.	
52	Cu with Ir wire	82 Ar/18 CO	73	-46.5	197	49	485	13	0.4	0.2	Uniform medium grey adherent. More shiny around edges and next to Ir wire. Small amount loose particulate.	

<sup>a</sup> Adherent deposit.<sup>b</sup> Weight gain/Total IrF<sub>6</sub> exposure.<sup>c</sup> Large amount loose powder.<sup>d</sup> Reactor cleaned.

## NOTES:

1. Very large aggregate lumps ~80  $\mu$ m.2. Approximately 5  $\mu$ m spears.3. Film appearance with some ~2  $\mu$ m lumps.4. Large lumps ~30  $\mu$ m and small lumps ~3  $\mu$ m.5. Very rough texture; particles ~30  $\mu$ m.6. Very rough texture; particles ~20 to 50  $\mu$ m.7. Film appearance with some ~10  $\mu$ m lumps.

8. Self-crystallized pure iridium; no preferred orientation.

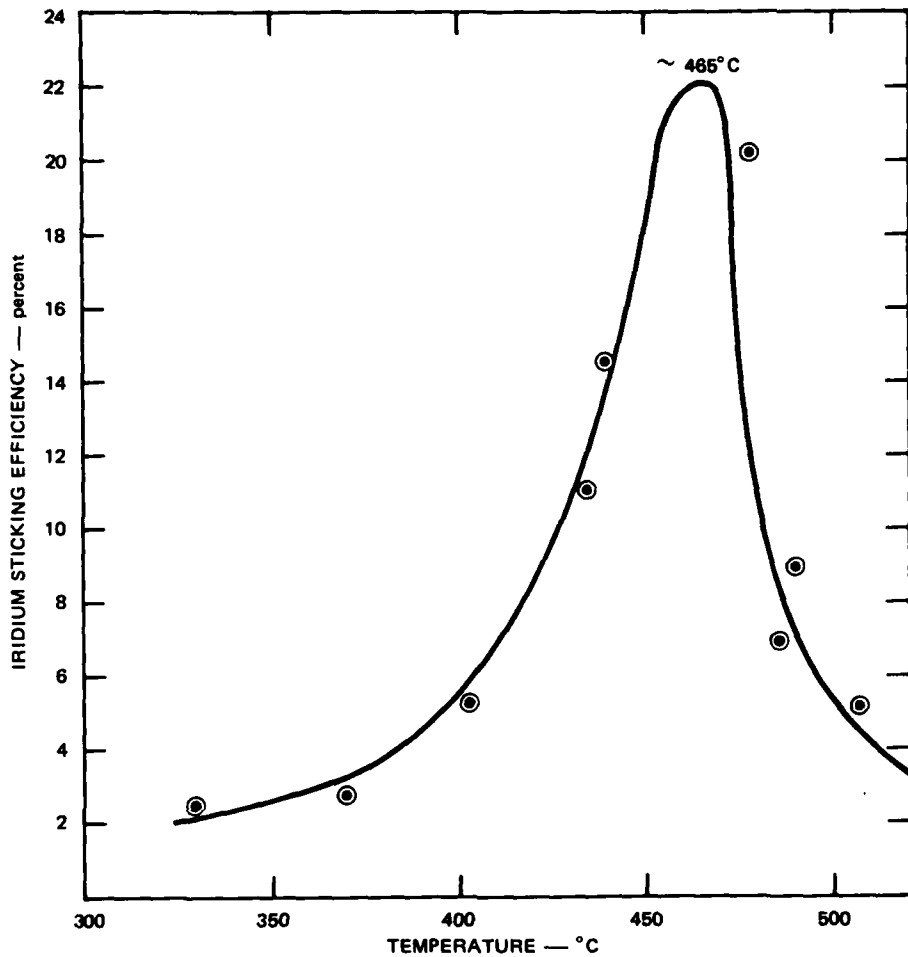


FIGURE 4 STICKING EFFICIENCY FOR IRIDIUM DEPOSITION ON COPPER FROM  $\text{IrF}_6$  AS A FUNCTION OF TEMPERATURE

#### D. Substrate Type

Several substrate materials for the deposition of iridium from  $\text{IrF}_6$  were investigated. These included copper, molybdenum, quartz, and iridium-coated copper disks [0.625-inch (1.5625 mm) diameter x 0.0005 inch (0.125 mm) thick], and copper-coated and  $\text{SiO}_2$ -coated silicon specimens.

For all samples except the copper and iridium surfaces, a substrate weight loss was observed during exposure to  $\text{IrF}_6$ . This can probably be ascribed to  $\text{IrF}_6$  attack to form volatile substrate species such as  $\text{MoF}_6$ ,  $\text{Mo}(\text{CO})_6$ , and  $\text{SiF}_4$ . For the copper substrate, initial reaction probably forms a passivation coating of nonvolatile  $\text{CuF}$  or  $\text{CuF}_2$ , which have melting points in excess of  $900^\circ\text{C}$ .

#### E. $\text{IrF}_6$ Exposure

The gas phase concentration of  $\text{IrF}_6$  in the carrier stream was varied by changing the temperature of the vaporizer. The total  $\text{IrF}_6$  mass flow rate was calculated from a knowledge of exposure time and the weight of the vaporizer before and after a deposition experiment. During initial experiments (Table 3), poor temperature control of the vaporizer resulted in a large variation of the  $\text{IrF}_6$  mass flow rate:  $168 \pm 149$  (standard deviation) mg/h at  $-46.5^\circ\text{C}$ . We speculate that the reason for the variation was nonuniform cooling of the solid  $\text{IrF}_6$  residing in the upper portion of the exit arms of the U-tube vaporizer. The  $\text{IrF}_6$  vaporizer was loaded with the gas stream entering the arm of the U-tube that eventually became the exit during the deposition process. Since the  $\text{IrF}_6$  readily condenses at  $-78^\circ\text{C}$ , it collected near the entrance. Consequently, the temperature of the vaporizer was sensitive to the depth of the coolant on that region of the U-tube. The difficulty was eliminated by reversing the direction of loading to correspond to the direction of vaporization, such that the  $\text{IrF}_6$  had to flow through the U-tube to enter the reactor and thermal uniformity was assured, and more uniform mass flow rates were achieved:  $62 \pm 21$  (standard deviation) mg/h at  $-46.5^\circ\text{C}$ .

By adjusting the temperature of the  $\text{IrF}_6$  vaporizer and the time for the experiment, total exposures were varied from ~20 to 3,000 mg  $\text{IrF}_6$ , and mass flow rates from ~1 to 470 mg/h. (Tables 3 and 4.) The results of this study showed that the quantity and quality of iridium deposited by CVD under these conditions is not strongly influenced by the rate at which  $\text{IrF}_6$  is supplied to the substrate surface. While larger  $\text{IrF}_6$

exposures result in the deposition of more iridium, the deposition efficiency remained essentially constant for a given temperature. In fact, the deposition efficiency curve constructed from the wide range of  $\text{IrF}_6$  exposures given in Table 3 is essentially the same as the curve from a narrower range of exposures in Table 4 (Figure 4).

#### F. Effect of Carrier Gas Composition and Flow Rate

Carrier gas effects were investigated using mixtures of argon, CO, and hydrogen supplied through calibrated flowmeters. Initial results (Table 3) demonstrated that the presence of CO aids in achieving an adherent iridium deposit on a copper substrate. For example, in a carrier stream of pure argon, a "sticking efficiency" of 2.6 percent was observed (Run 13); at nearly the same temperature in the presence of (18 CO)/(82 argon) volume percent (vol%), 16.6 of the  $\text{IrF}_6$  was deposited on the substrate (Run 5). Hydrogen is apparently too strong a reducing agent; in the presence of (18 hydrogen)/(82 argon) vol%, a large amount of nonadherent iridium powder was formed on the surface of the substrate (Run 49).

The nature of the iridium deposit on a copper substrate is affected by the concentration of CO in the CO/argon carrier stream. In the presence of 40 vol% CO, most of the deposit is in the form of loose powder, probably generated during gas phase reduction of  $\text{IrF}_6$  above the substrate surface. When the CO concentration is lowered to 12 vol%, deposition efficiency is poor and little powder forms. While the effect of CO was not optimized over a broad range of concentrations, it appeared that iridium was deposited in the presence of 18 vol% CO in argon in the form of an adherent coating.

The effect of total gas-flow rate was not extensively studied. Most deposition experiments were conducted at a volumetric flow rate of  $73 \text{ cm}^3/\text{min}$ . Lowering the flow rate to  $50 \text{ cm}^3/\text{min}$  appeared to have little effect on deposition efficiency and quality of the iridium deposit.

At a high flow rate of 220 cm<sup>3</sup>/min, however, a reduction in deposition efficiency from about 20 to 4 was observed.

#### G. Effect of Low Pressure

Chemical vapor deposition studies are frequently conducted at low pressure to achieve desirable results. In the present study we evaluated 0.30- and 0.1-atm conditions using a Cartesian diver manostat and a deposition temperature near the maximum shown in Figure 4. While the composition of the carrier gas was adjusted to the ratio (18 CO)/(82 argon), it was not possible to measure the total volumetric flow rate at subambient pressure. Under these conditions we observed little if any iridium deposit on the copper substrate (Table 4, Run 40-44).

#### H. Nature of the Deposit

To evaluate the effectiveness of our experimental approach to optimizing the deposition of iridium from IrF<sub>6</sub> on a copper substrate, the deposit was analyzed in terms of

- Sticking efficiency
- Weight of adherent deposit
- Visual appearance
- Scanning electron microscopy and X-ray fluorescence analysis
- X-ray diffraction analysis.

Sticking Efficiency--Evaluation of parameters to maximize the amount of iridium deposition was most easily expressed in terms of the sticking efficiency for IrF<sub>6</sub>. In our work, sticking efficiency was influenced most by temperature and to a lesser degree by carrier-gas composition and flow rate. The repeatable observation of a narrow-range temperature dependence for iridium deposition, peaking at about 465°C (Figure 4), was a significant result from our study.

Weight of Adherent Deposit--In several cases, particularly in the presence of a high concentration of CO and hydrogen, a large amount of

loose iridium powder was found on the substrate surface. Powder formation probably occurs in the gas phase and is not a function of the nature of the surface. All results are reported in terms of the weight of adherent iridium deposit and not loose powder, which can easily be removed by tilting the sample. Under optimized conditions of temperature (~465°C) and carrier-gas composition [(18 CO)/(82 argon) vol%], more than 200 mg of adherent iridium was deposited on a 198 mm<sup>2</sup> copper disk in 4 hours. Presumably, larger amounts could be deposited over longer time periods.

Visual Appearances--As shown in Tables 3 and 4, the visual appearance of the iridium deposits from IrF<sub>6</sub> ranges in color from silver to black, suggesting a variety of particle sizes. In general, thinner deposits tended to be more silver/grey in color, but no particular hue could be related to a given parameter such as temperature, flow rate, or gas composition.

Microscopic Examination--Selected iridium deposits were examined by scanning electron microscopy (SEM). Most samples appeared to be dendritic (Figure 5) in nature, but occasionally a film was formed (Figure 6). The variation in morphology of the iridium deposits suggest that deposition is quite sensitive to subtle changes in experimental conditions, which we were not able to control repeatably. We speculate that temperature control to better than  $\pm 5^{\circ}\text{C}$  may be required to achieve consistent morphology. SEM analysis further suggests that the initial layers of iridium deposited on copper appear as a thin film, followed by particulate or dendritic growth. This conclusion was reached by examining the iridium interface of a particulate-type deposit (Figure 7) after removal from the copper substrate. Figure 8 is a SEM photograph of the copper side of the iridium deposit, which appears film-like in nature. It is possible, however, that acid treatment used to remove the iridium deposit from the substrate may have produced the effect shown.

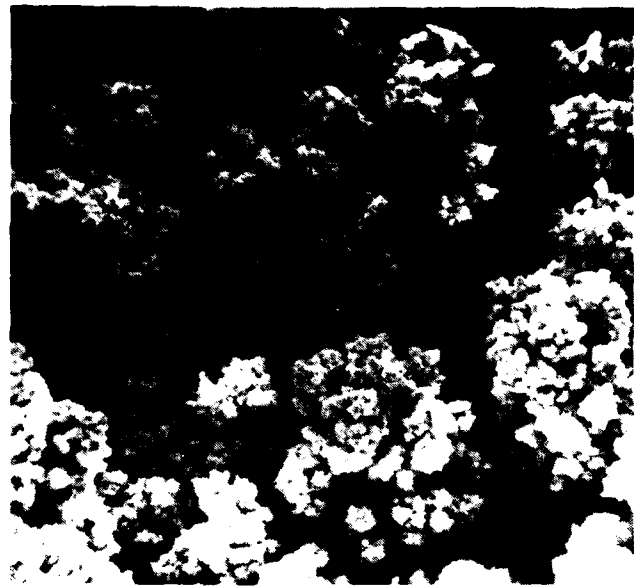


FIGURE 5 DENDRITE IRIDIUM DEPOSIT (RUN 33 IN TABLE 4)



FIGURE 6 5000 $\times$  SEM PHOTOGRAPH OF IRIDIUM DEPOSIT ON COPPER SUBSTRATE (RUN 16 IN TABLE 3)

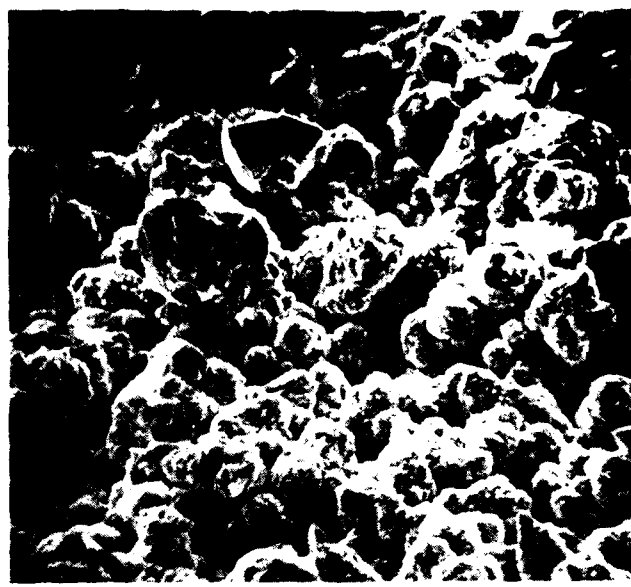


FIGURE 7 5000 $\times$  SEM PHOTOGRAPH OF IRIDIUM DEPOSIT ON COPPER SUBSTRATE (RUN 5 IN TABLE 3) BEFORE REMOVAL



FIGURE 8 2000 $\times$  SEM PHOTOGRAPH OF IRIDIUM DEPOSIT (BACK SIDE, RUN 5 IN TABLE 3) AFTER REMOVAL FROM COPPER SUBSTRATE  
XRF analysis shows minor copper contamination

I. Elemental Analysis

X-ray fluorescence and diffraction analyses of selected deposits demonstrated the presence of essentially pure iridium with occasional trace contamination from aluminum and chlorine. X-ray diffraction analysis showed no preferred crystallographic orientation for any of the deposits studied.

J. Deposition on Silicon Microstructures

We attempted to deposit a microporous film on a silicon substrate supplied by Richard Thomas of NRL. The structure was prepared by anisotropic etching of a <110> silicon wafer to produce a pattern of ridges about 60- $\mu\text{m}$  high, 14- $\mu\text{m}$  long, and 1- $\mu\text{m}$  wide, spaced 6  $\mu\text{m}$  apart in rows separated by 30  $\mu\text{m}$ . The pattern is apparent in Figure 9, which also shows the nature of the resultant deposit. The substrate was coated with copper by vacuum evaporation prior to iridium deposition. The dendritic growth, similar to that shown in Figure 5, totally dominated the deposition process.

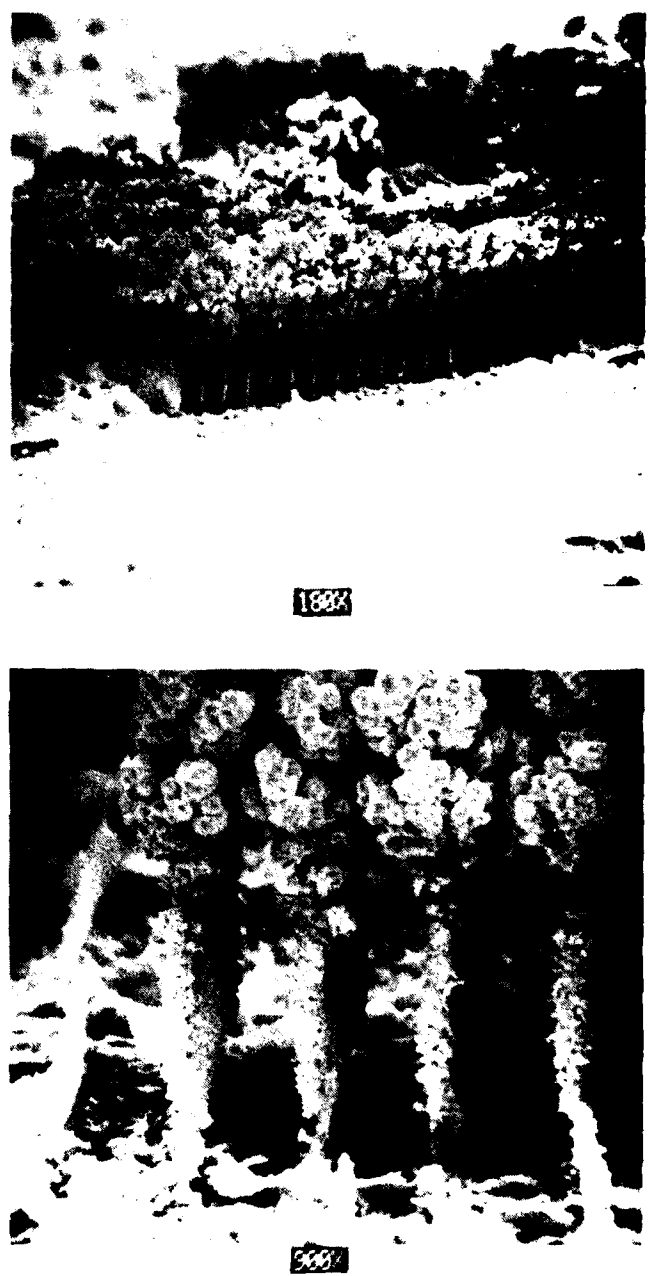


FIGURE 9 DEPOSITION ON SILICON MICROSTRUCTURE

#### IV DISCUSSION

##### A. Iridium Deposition from IrCl<sub>3</sub>

A computer-assisted literature search for thermodynamic and vapor pressure properties of IrCl<sub>3</sub> produced little pertinent data on which to base volatilization and deposition experiments. Powell (1962) suggested that the volatilization and decomposition temperatures of IrCl<sub>3</sub> are too close to permit efficient use of this material in vapor deposition reactions, but that metal carbonyl halide compounds are stable and amenable for CVD work. Macklin and Withers (1967) reported on the deposition of iridium from IrCl<sub>3</sub>, but presented little data on the nature of the volatile iridium species or the amount of iridium deposited. We speculate that for iridium carbonyl chloride species, such IrCOCl<sub>2</sub> may be formed in the presence of IrCl<sub>3</sub> and CO (Powell, 1962). Our results, however, suggest that (IrCOCl<sub>3</sub>) generated from IrCl<sub>3</sub> and CO is not an efficient transport reagent for iridium CVD work, because of the narrow-range temperature limits for its formation and decomposition.

##### B. Iridium Deposition from IrF<sub>6</sub>

A review of the work of Macklin and Withers (1967) suggested that IrF<sub>6</sub> is the best halide for depositing iridium coatings. The hexafluoride, which has a sublimation pressure of 1 atm at 53°C, is the most volatile source of the metal (vapor pressure = 248 torr at 25°C, 77 torr at 0°C, and 7 torr at -40°C), but is quite sensitive to decomposition. This sensitivity creates a handling and storage problem that requires careful attention to cleanliness and the avoidance of reducing agents. In practice, it is nearly impossible to avoid the slow decomposition of the hexafluoride to iridium metal or IrF<sub>6</sub> species. In our work, IrF<sub>6</sub> was prepared and stored in fluorine-passivated apparatus, and between runs maintained at -78.5°C.

While Macklin and Withers (1967) reported that iridium deposition rates up to 0.5 mil/h (13  $\mu\text{m}/\text{h}$ ) were observed using  $\text{IrF}_6$ , they report little data to support this claim. We estimate from their work that the iridium layer deposited on a graphite surface is about 2.3  $\mu\text{m}$  thick.

During the course of our investigation, we were able to achieve deposits considerably thicker than previously reported. For example, the thickness of the film-like deposit shown in Figure 6 is calculated from its weight and surface area to be about 50  $\mu\text{m}$  and was deposited at about 13  $\mu\text{m}/\text{h}$  (in agreement with the rate reported by Macklin and Withers). Other deposits, which are probably porous in nature, were generally greater than 10  $\mu\text{m}$ .

The narrow-range temperature dependence for iridium deposition from  $\text{IrF}_6$  (Figure 4) has not been previously reported. We speculate that the temperature dependence curve could be refined with more-accurate and precise temperature measurement and control than is possible with the present apparatus.

Sladek (1971) mathematically described the temperature region in chemical vapor deposition for the transition from film to particle formation. In Sladek's scheme, the transition occurs rather suddenly at critical values defined as  $M^*$  and  $T_0^*$ , and (in general) film formation is favored at lower temperatures. We do not have sufficient critical information concerning the physical/chemical properties of  $\text{IrF}_6$  to calculate  $M^*$  and  $T_0^*$  for a theoretical approach to the problem. It seems clear, however, that this approach would not predict a maximum in the sticking efficiency curve (Figure 4) and that this effect is indeed unique to chemical vapor deposition of iridium from  $\text{IrF}_6$ .

## REFERENCES

- Bassous, E., 1978: "Fabrication of Novel Three-Dimensional Microstructures by Anisotropic Etching of <100> and <110> Silicon," IEEE Trans. on Electron Dev., Vol. ED-25, No. 10, pp. 1178-1185.
- Bauer, E., 1962: "Fiber Texture," Trans. 9th AVS Vac. Symp., p. 35 (McMillan Co., New York).
- Brodie, I., and R.O. Jenkins, 1956: "Impregnated Barium Dispenser Cathodes Containing Strontium or Calcium Oxide," J. Appl. Phys., Vol. 27, No. 4, pp. 417-418 (April).
- Brodie, I., and R.O. Jenkins, 1957a: "Evaporation of Barium from Impregnated Cathodes," J. Electronics, Vol. 2, No. 5, pp. 457-476 (March).
- Brodie, I., and R.O. Jenkins, 1957b: "The Nature of the Emitting Surface of Barium Dispenser Cathodes," Brit. J. Appl. Phys., Vol. 8, No. 1, pp. 27-29 (January).
- Falce, L.R., 1978: "Iridium Cathode Development," Final Report, Varian Associates, N00713-77-C-0186, Naval Research Laboratories.
- Levi, R., 1955: "Improved Impregnated Cathode," J. Appl. Phys., Vol. 26, No. 5, p. 639 (May).
- Longo, R., 1978: "Dispenser Cathodes for Space Applications," Tri-Service Cathode Workshop, Naval Research Laboratories, Arlington, Virginia (January).
- Macklin, B.A., and J.C. Withers, 1967: "The Chemical Vapor Deposition of Iridium," Proc. Conf. Chem. Vap. Dep. of Refractory Metals, Alloys, and Compounds, Gatlinburg, Tennessee, p. 161.

Maloney, C., 1978: "SEM and AES Studies on Cathodes," Tri-Service Cathode Workshop, Naval Research Laboratories, Arlington, Virginia.

McMurray, N.D., R.H. Singleton, K.W. Muszar, and D.R. Zimmerman, 1965: "Tungsten Thermionic Emitter Surfaces Improved by Chemical Vapor Deposition," J. Metals, No. 17, p. 600.

Powell, C.F., I.E. Campbell, and B.W. Conser, 1962: Vapor Plating (John Wiley and Sons, Inc. New York).

Powell, C.F., J.H. Oxley, and J.M. Blocher, Jr., 1966: Vapor Deposition (John Wiley and Sons, New York).

Rittner, E.S., W.C. Rutledge, and R.H. Ahlert, 1957: "On the Mechanism of Operation of the Barium Aluminate Impregnated Cathode," J. Appl. Phys., Vol. 28, No. 12, pp. 1468-1473 (December).

Schroff, A.M., 1978: "Lifetimes of Matrix Cathodes," Tri-Service Cathode Workshop, Naval Research Laboratories, Arlington, Virginia (January).

Sickafus, E., 1978: "Space Dispenser Cathodes," Tri-Service Cathode Workshop, Naval Research Laboratories, Arlington, Virginia (January).

Sladek, K.J., 1971: "The Role of Homogeneous Reactions in Chemical Vapor Deposition," J. Electrochem. Soc., Vol. 118, No. 4, p. 654.

Smith, D.H., 1978: "Lifetimes of Impregnated Cathodes," Tri-Service Cathode Workshop, Naval Research Laboratories, Arlington, Virginia (January).

Thomas, R.E., T. Pankey, J.W. Gibson, and G.A. Haas, in press: "Thermionic Properties of BaO on Iridium," preprint.

Tuck, R., 1978: "Physical Processes in Dispenser Cathodes," Tri-Service Cathode Workshop, Naval Research Laboratories, Arlington, Virginia (January).

Weinstock, B., 1964: Chem. & Engr. News, p. 86, (21 September).

Weissman, I., and M.L. Kinter, 1963: "Improved Thermionic Emitter Using Uniaxially Oriented Tungsten," J. Appl. Phys., Vol. 34, p. 3187.

Yang, J., and R.G. Hudson, 1967: "Evaluation of Chemically Vapor Deposited Tungsten as Electron Emitters for Nuclear Thermionic Application," Proc. Conf. Chemical Vapor Deposition of Refractory Metals, Alloys, and Compounds, Gatlinburg, Tennessee, p. 329.

D  
FI  
IO